Supporting Information

Thermo- and Mechanical-Grinding-Triggered Color and Luminescence Switches of Diimine-Platinum(II) Complex with 4-Bromo-2,2'-Bipyridine

Jun Ni,[*a, b] You-Gui Wang,[a] Hui-Hui Wang,[a] Liang Xu,[a] Yan-Qiu Zhao,[a] Yu-Zhen Pan[a] and Jian-Jun Zhang[a]

[a]*College of Chemistry, Dalian University of Technology, 2 Lingshui Road, Dalian 116023, China,*

[b]*State Key Laboratory of Structural Chemistry, Fujian Institute of Research on the Structure of Matter, Chinese Academy of Sciences, Fuzhou, Fujian 350002, China.*

Contents

Table S1. Crystal data and structure refinement of **1**·2(CH_2Cl_2) and **1**·2($CHCl_3$).

	1·2(CH_2Cl_2)	**1**·2($CHCl_3$)
Empirical formula	$C_{28}H_{21}BrCl_4N_2Pt$	$C_{28}H_{19}BrCl_6N_2Pt$
M	802.27	871.15
Crystal system	monoclinic	monoclinic
Space group	$P2_1/c$	$P2_1/c$
a / Å	7.684(2)	7.7725(4)
b / Å	22.104(3)	21.7699(12)
c / Å	17.567(3)	18.8391(8)
α / °	90	90
β / °	95.756(2)	94.510(2)
γ / °	90	90
V / Å^3	2968.7(10)	3177.8(3)
Z	4	4
D_c /g.cm^{-3}	1.795	1.819
μ(mm^{-1})	6.453	6.198
Radiation (λ, Å)	0.71073	0.71073
T / K	296	296
F(000)	1536	1660
R_{int}	0.075	0.034
Reflections collected / uniques	14368 / 5202	14104 / 5562
Observed reflections ($I > 2\sigma(I)$)	3299	4055
$R1^a$($I > 2\sigma(I)$)	0.0546	0.0568
$wR2^b$(all data)	0.1482	0.1740
GOF	1.007	1.042

$^a R1 = \Sigma|F_o - F_c|/\Sigma F_o$, $^b wR2 = \Sigma[w(F_o^2 - F_c^2)^2]/\Sigma[w(F_o^2)]^{1/2}$

Table S2. Selected bond lengths (Å), bond angles (º) and shortest Pt···Pt (Å) distances for **1**·2(CH_2Cl_2) and **1**·2($CHCl_3$).

	1·2(CH_2Cl_2)	**1**·2($CHCl_3$)
Shortest Pt···Pt distance	4.911	4.982
Pt1-N	2.066(9)	2.070(8)
	2.063(9)	2.074(9)
Pt1-C	1.966(13)	1.971(12)
	1.941(12)	1.973(13)
N-Pt1-N	79.3(4)	78.6 (4)
C-Pt1-N	93.9(4)	95.6(4)
C-Pt1-N	95.1(4)	94.0(4)
C-Pt1-C	91.7(4)	9.18(4)

Table S3 Hydrogen-bonding geometry (Å,°) and short interactions for **1**·2(CH_2Cl_2) and **1**·2($CHCl_3$).

1·2(CH_2Cl_2)					
D-H···*A*	*D*-H	H···*A*	*D*···*A*	*D*-H···*A*	Symmetry code
C01-H01A…π(C19≡C20)	0.97	2.86	3.414	117	x,y,z
C01-H01B…π(C11≡C12)	0.97	2.66	3.628	174	x,y,z
C16-H16…Br1	0.93	2.97	3.566	123	1-x,1/2+y,3/2-z
	center…center				center…center
π(Cg1)…π(Cg3')	3.956		π(C11≡C12)…π(Cg2)		3.403
Cg1 is the pyridine ring containing N2 atom, Cg2 is the pyridine ring containing N1, Cg3' is the benzene ring containing C13 with symmetry code (1-x,1-y,1-z).					
1·2($CHCl_3$)					
D-H···*A*	*D*-H	H···*A*	*D*···*A*	*D*-H···*A*	Symmetry code
C01-H01…π(C11≡C12)	0.98	2.73	3.554	142	x,y,z
C01-H01…π(C19≡C20)	0.98	2.86	3.594	132	x,y,z
C02-H02…π(Cg)	0.98	2.71	3.648	162	1-x,-1/2+y,3/2-z
Br1…Cl3	3.367 (x,y,z)		Br1'…Cl3		3.489 (x,3/2-y,-1/2+z)
	center…center				center…center
π(Cg1)…π(Cg3')	3.978		π(C19≡C20)…π(Cg2)		3.420
Cg is the benzene ring containing C13 atom, Cg1 is the pyridine ring containing N1 atom, Cg2 is the pyridine ring containing N2, Cg3' is the benzene ring containing C21 with symmetry code (-x,1-y,1-z).					

Table S4. The optimized coordinates of **1** monomer by DFT method at the PBE1PBE level.

Atom	Coordinates (Angstroms)		
	X	Y	Z
Pt	0.34075100	-0.33008000	-0.01064000
Br	-6.37105900	-0.07428600	0.05513000
C	0.70603200	1.57184000	-0.00161000
N	-0.27078000	-2.32673900	-0.03206000
C	1.04188400	4.20089000	0.02708000
N	-1.73628900	-0.14275900	-0.00582000
C	-3.77845800	1.09360300	0.03348000
H	-4.27810800	2.05466300	0.05154000
C	2.24176100	-0.69610100	-0.00478000
C	-1.60933100	-2.52916900	-0.03602000
C	-2.42880000	-1.30516800	-0.01131000
C	1.42585600	6.98494900	0.09412000
H	1.57497600	8.06061900	0.11972000
C	4.82027000	-1.30632300	-0.01454000
C	-1.27517200	-4.90681900	-0.08757000
H	-1.67241300	-5.91661900	-0.11034000
C	3.42850000	-1.00253200	0.00176000
C	0.84714300	2.78926000	0.00072000
C	-2.13698100	-3.81847800	-0.06412000
H	-3.20936100	-3.97428800	-0.06962000
C	0.09724800	-4.68143000	-0.08286000
H	0.80628800	-5.50168000	-0.10170000
C	-3.82148000	-1.31149700	0.00675000
H	-4.37892000	-2.23936700	0.00539000
C	7.07662100	-0.78032400	-0.74215000
H	7.75564100	-0.13528500	-1.29319000

C	-4.49533900	-0.09820700	0.02906000
C	5.71937100	-0.48666300	-0.72022000
H	5.33196100	0.38024700	-1.24616000
C	-2.39485800	1.02297200	0.01631000
H	-1.76197800	1.90711100	0.02082000
C	0.63936500	6.40908000	-0.90148000
H	0.17411600	7.03594000	-1.65753000
C	0.56195900	-3.37471000	-0.05541000
H	1.61800900	-3.11800100	-0.05218000
C	1.83633400	4.79419900	1.02418000
H	2.30296400	4.15639900	1.76836000
C	2.02237500	6.17034900	1.05468000
H	2.63993500	6.61050900	1.83296000
C	0.44653400	5.03363000	-0.93654000
H	-0.16070600	4.58329000	-1.71625000
C	6.69024900	-2.71034400	0.64457000
H	7.06645900	-3.57686400	1.18184000
C	7.56964000	-1.89208500	-0.06144000
H	8.63204000	-2.11787500	-0.07918000
C	5.33104000	-2.42398300	0.66839000
H	4.64649900	-3.05772300	1.22476000

Table S5. Partial molecular orbital compositions (%) in the ground state for **1** in dichloromethane solution by TD-DFT method at the PBE1PBE level.

Orbital	Energy (eV)	MO Contribution (%)		
		Pt	4-Br-2,2'-bipyridine	C≡CPh
LUMO+10	0.41	53.4(24/33/43)	21.9	24.7
LUMO+5	-0.14	9.4(77/10/13)	80.8	9.8
LUMO+4	-0.34	4.9(9/22/69)	6.0	89.1
LUMO+3	-0.57	15.6(0/68/32)	6.2	78.2
LUMO+2	-1.31	1.7(0/26/74)	97.3	1.0
LUMO+1	-1.61	2.4(0/66/34)	96.4	1.2
LUMO	-2.59	4.4(0/47/53)	92.5	3.1
HOMO	-5.75	17.7(0/0/99)	1.6	80.7
HOMO-1	-5.97	15.8(0/5/94)	4.1	80.1
HOMO-2	-6.34	32.1(0/1/99)	3.3	64.6
HOMO-3	-6.68	18.7(0/2/98)	5.4	75.9
HOMO-4	-6.91	96.2(38/0/72)	0.7	3.1
HOMO-5	-7.14	0(26/9/65)	0	100
HOMO-7	-7.67	19.3(0/1/99)	49.3	31.4
HOMO-8	-7.79	11.7(0/0/99)	69.2	19.1
HOMO-9	-7.98	19.9(0/1/99)	9.6	70.5

Table S6. Absorption and emission transition properties of **1** in dichloromethane solution by TD-DFT method at the PBE1PBE level with the polarized continuum model (PCM).

States	*E*, nm (eV)	O.S.	Component	Contri.	Assignment	Measured Wavelength (nm)
T_1	539 (2.30)	0.0000	HOMO→LUMO	96%	^{3}LLCT/^{3}MLCT	580
T_2	499 (2.49)	0.0000	HOMO-1→LUMO	92%	^{3}LLCT/^{3}MLCT	
S_1	511 (2.43)	0.0538	HOMO→LUMO	100%	^{1}LLCT/^{1}MLCT	
S_2	463 (2.68)	0.1954	HOMO-1→LUMO	100%	^{1}LLCT/^{1}MLCT	450
S_3	432 (2.87)	0.0391	HOMO-2→LUMO	100%	^{1}LLCT/^{1}MLCT	415
S_8	330 (3.75)	0.1281	HOMO→LUMO+2	80%	^{1}LLCT/^{1}MLCT	
			HOMO-1→LUMO+1	18%	^{1}LLCT/^{1}MLCT	
S_{14}	289 (4.29)	0.8981	HOMO→LUMO+3	49%	^{1}IL/^{1}MC	290
			HOMO-7→LUMO	46%	^{1}LLCT/^{1}MLCT/^{1}IL	
			HOMO-2→LUMO+2	5%	^{1}LLCT/^{1}MLCT	
S_{18}	284 (4.37)	0.3063	HOMO-8→LUMO	74%	^{1}LLCT/^{1}MLCT/^{1}IL	
			HOMO-3→LUMO+1	23%	^{1}LLCT/^{1}MLCT	
S_{19}	274 (4.53)	0.1053	HOMO-2→LUMO+3	46%	^{1}IL/^{1}MC	
			HOMO-1→LUMO+3	29%	^{1}IL/^{1}MC	
			HOMO-3→LUMO+2	15%	^{1}LLCT/^{1}MLCT	
S_{21}	271 (4.57)	0.3061	HOMO-1→LUMO+3	33%	^{1}IL/^{1}MC	
			HOMO→LUMO+4	20%	^{1}IL	
			HOMO-3→LUMO+2	18%	^{1}LLCT/^{1}MLCT	
			HOMO-2→LUMO+3	13%	^{1}IL/^{1}MC	
			HOMO-9→LUMO	11%	^{1}LLCT/^{1}MLCT	

S_{26}	257 (4.81)	0.2530	HOMO→LUMO+4	31%	^{1}IL	269
			HOMO→LUMO+10	21%	^{1}MC/^{1}MLCT/^{1}LLCT/ ^{1}IL	
			HOMO→LUMO+5	21%	^{1}LLCT/^{1}MLCT	
			HOMO-9→LUMO	11%	^{1}LLCT/^{1}MLCT	
			HOMO-3→LUMO+3	7%	^{1}IL/^{1}MC	

IL denotes intraligand $\pi\rightarrow\pi^*$ transition of 4-Br-2,2'-bipyridine or $C\equiv CC_6H_5$ ligand; LLCT denotes $\pi(C\equiv CC_6H_5)\rightarrow \pi^*$(4-Brbpy) state; MLCT denotes $5d$(Pt)$\rightarrow\pi^*$(4-Brbpy) state; MC denotes metal-centered transition.

Table S7. Partial molecular orbital compositions (%) in the ground state for solid-state **1**·2(CH_2Cl_2) by TD-DFT method at the PBE1PBE level.

Orbital	Energy (eV)	MO Contribution (%)		
		Pt (s/p/d)	4-Br-2,2'-bipyridine	C≡CPh
LUMO+5	-1.20	2.9(45/31/24)	77.5	19.6
LUMO+4	-1.30	3.3(39/44/17)	94.2	2.5
LUMO+3	-1.50	3.1(4/62/33)	95.5	1.4
LUMO+2	-1.61	5.4(39/49/12)	92.5	2.1
LUMO+1	-2.38	3.9(11/24/65)	93.0	3.1
LUMO	-2.45	5.6(13/51/36)	90.6	3.8
HOMO	-5.44	19.0(0/2/98)	3.0	78.0
HOMO-1	-5.46	19.5(1/1/98)	2.4	78.1
HOMO-2	-5.69	22.2(0/5/95)	5.1	72.7
HOMO-3	-5.75	21.0(0/5/95)	5.1	74.0
HOMO-4	-6.06	31.4(2/2/96)	2.9	65.7
HOMO-5	-6.07	29.8(0/2/98)	3.1	67.1
HOMO-6	-6.45	78.6(28/0/72)	9.0	12.4
HOMO-7	-6.50	84.7(27/0/72)	8.5	6.8
HOMO-14	-7.14	28.7(0/0/99)	16.0	55.3
HOMO-15	-7.21	29.0(0/0/100)	14.0	57.0
HOMO-16	-7.42	42.9(0/0/100)	10.9	46.2

Table S8. Absorption and emission transition properties of **1**·2(CH_2Cl_2) by TD-DFT method at the PBE1PBE level with the polarized continuum model (PCM).

States	*E*, nm (eV)	O.S.	Component	Contri.	Assignment	Measured Wavelength (nm)
T_1	579 (2.14)	0.0000	HOMO→LUMO	81%	^{3}LLCT/^{3}MLCT	549
			HOMO-1→LUMO+1	19%	^{3}LLCT/^{3}MLCT	
T_2	574 (2.16)	0.0000	HOMO-1→LUMO	58%	^{3}LLCT/^{3}MLCT	
			HOMO→LUMO+1	42%	^{3}LLCT/^{3}MLCT	
S_1	541 (2.29)	0.0000	HOMO→LUMO	82%	^{1}LLCT/^{1}MLCT	
			HOMO-1→LUMO+1	14%	^{1}LLCT/^{1}MLCT	
S_2	535 (2.32)	0.0772	HOMO-1→LUMO	57%	^{1}LLCT/^{1}MLCT	505
			HOMO→LUMO+1	43%	^{1}LLCT/^{1}MLCT	
S_8	469 (2.64)	0.0967	HOMO-2→LUMO+1	72%	^{1}LLCT/^{1}MLCT	474
			HOMO-3→LUMO	15%	^{1}LLCT/^{1}MLCT	
S_{10}	444 (2.79)	0.0823	HOMO-5→LUMO	62%	^{1}LLCT/^{1}MLCT	420
			HOMO-4→LUMO+1	26%	^{1}LLCT/^{1}MLCT	
S_{32}	343 (3.61)	0.1296	HOMO-1→LUMO+4	38%	^{1}LLCT/^{1}MLCT	331
			HOMO-2→LUMO+3	29%	^{1}LLCT/^{1}MLCT	
			HOMO→LUMO+5	14%	^{1}LLCT/^{1}MLCT/^{1}IL	
			HOMO-5→LUMO+2	11%	^{1}LLCT/^{1}MLCT	
S_{51}	308 (4.01)	0.0451	HOMO-14→LUMO	43%	^{1}LLCT/^{1}MLCT	312
			HOMO-4→LUMO+5	18%	^{1}LLCT/^{1}MLCT/^{1}IL	
			HOMO-5→LUMO+4	16%	^{1}LLCT/^{1}MLCT/^{1}IL	
			HOMO-15→LUMO+1	10%	^{1}LLCT/^{1}MLCT/^{1}IL	
S_{56}	299 (4.15)	0.0383	HOMO-6→LUMO+3	36%	^{1}LLCT/^{1}MLCT	301
			HOMO-7→LUMO+4	22%	^{1}LLCT/^{1}MLCT	
			HOMO-7→LUMO+2	15%	^{1}MLCT	
			HOMO-16→LUMO	10%	^{1}LLCT/^{1}MLCT/^{1}IL	

Table S9. Partial molecular orbital compositions (%) in the ground state for solid-state **1**·2($CHCl_3$) by TD-DFT method at the PBE1PBE level.

Orbital	Energy (eV)	MO Contribution (%)		
		Pt (s/p/d)	4-Br-2,2'-bipyridine	C≡CPh
LUMO+5	-0.86	3.2(41/33/26)	94.2	2.6
LUMO+4	-1.04	6.6(30/58/12)	89.4	4.0
LUMO+3	-1.61	2.4(11/55/34)	95.3	2.3
LUMO+2	-1.63	2.8(37/43/20)	97.2	2.3
LUMO+1	-2.43	4.1(13/19/67)	93.7	2.2
LUMO	-2.52	5.8(13/49/38)	90.1	4.1
HOMO	-5.55	18.6(1/2/97)	2.4	79.0
HOMO-1	-5.57	18.8(1/1/98)	1.8	79.4
HOMO-2	-5.76	21.8(0/5/95)	6.0	72.2
HOMO-3	-5.79	22.3(0/6/94)	5.0	72.7
HOMO-4	-6.15	33.1(3/2/95)	3.6	63.3
HOMO-5	-6.17	31.6(0/2/97)	3.1	65.3
HOMO-6	-6.46	82.6(27/0/72)	10.5	6.9
HOMO-7	-6.50	86.2(27/0/73)	9.5	4.3
HOMO-9	-6.63	9.7(7/4/89)	2.6	87.7
HOMO-12	-6.98	0.7(2/4/94)	0.2	99.1
HOMO-14	-7.33	33.9(1/0/99)	16.9	49.2
HOMO-16	-7.40	31.6(0/0/99)	12.3	56.1
HOMO-17	-7.52	45.0(0/0/100)	10.0	45.0

Table S10. Absorption and emission transition properties of **1**·2($CHCl_3$) by TD-DFT method at the PBE1PBE level with the polarized continuum model (PCM).

States	*E*, nm (eV)	O.S.	Component	Contri.	Assignment	Measured Wavelength (nm)
T_1	568 (2.18)	0.0000	HOMO→LUMO	80%	^{3}LLCT/^{3}MLCT	549
			HOMO-1→LUMO+1	15%	^{3}LLCT/^{3}MLCT	
T_2	561 (2.21)	0.0000	HOMO-1→LUMO	58%	^{3}LLCT/^{3}MLCT	
			HOMO→LUMO+1	42%	^{3}LLCT/^{3}MLCT	
S_1	534 (2.32)	0.0000	HOMO→LUMO	88%	^{1}LLCT/^{1}MLCT	
			HOMO-1→LUMO+1	12%	^{1}LLCT/^{1}MLCT	
			HOMO-3→LUMO	4%	^{1}LLCT/^{1}MLCT	
S_2	529 (2.34)	0.0721	HOMO-1→LUMO	70%	^{1}LLCT/^{1}MLCT	497
			HOMO→LUMO+1	30%	^{1}LLCT/^{1}MLCT	
S_5	483 (2.56)	0.0769	HOMO-2→LUMO	74%	^{1}LLCT/^{1}MLCT	
			HOMO→LUMO+1	13%	^{1}LLCT/^{1}MLCT	
			HOMO-1→LUMO	11%	^{1}LLCT/^{1}MLCT	
S_8	463 (2.68)	0.0526	HOMO-3→LUMO+1	81%	^{1}LLCT/^{1}MLCT	465
S_{10}	439 (2.83)	0.0943	HOMO-5→LUMO	67%	^{1}LLCT/^{1}MLCT	420
			HOMO-4→LUMO+1	21%	^{1}LLCT/^{1}MLCT	
			HOMO-3→LUMO+1	8%	^{1}LLCT/^{1}MLCT	
S_{18}	374 (3.31)	0.0606	HOMO-6→LUMO+1	54%	^{1}IL/^{1}MLCT	
			HOMO-7→LUMO	40%	^{1}MLCT	
S_{26}	355 (3.49)	0.0921	HOMO-2→LUMO+2	52%	^{1}LLCT/^{1}MLCT	
			HOMO-9→LUMO+1	27%	^{1}LLCT	
			HOMO-3→LUMO+3	15%	^{1}LLCT/^{1}MLCT	
S_{34}	325 (3.82)	0.0281	HOMO-1→LUMO+4	73%	^{1}LLCT/^{1}MLCT	329
			HOMO-2→LUMO+4	20%	^{1}LLCT/^{1}MLCT	

S_{37}	315 (3.93)	0.0491	HOMO-2→LUMO+4	72%	^{1}LLCT/^{1}MLCT	312
			HOMO-1→LUMO+4	23%	^{1}LLCT/^{1}MLCT	
S_{47}	304 (4.08)	0.0387	HOMO-14→LUMO	54%	^{1}LLCT/^{1}MLCT/^{1}IL	302
			HOMO-12→LUMO	20%	^{1}LLCT	
			HOMO-16→LUMO+1	15%	^{1}LLCT/^{1}MLCT/^{1}IL	
			HOMO-17→LUMO	7%	^{1}LLCT/^{1}MLCT/^{1}IL	
			HOMO-3→LUMO+5	4%	^{1}LLCT/^{1}MLCT	

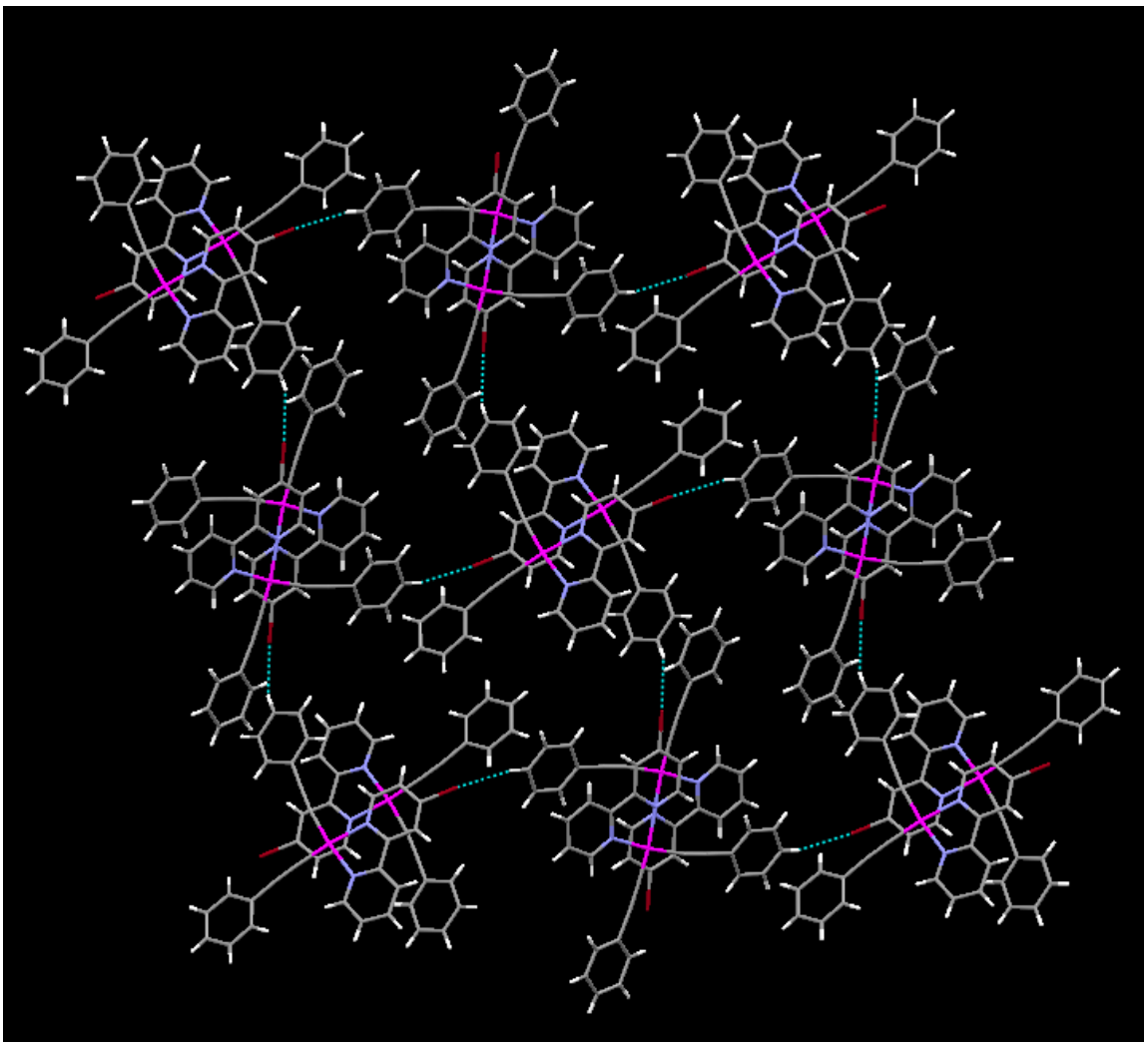

Figure S1. The Pt moiety plane in **1**·2(CH_2Cl_2), observed from *a* axis direction. The solvate molecules are omitted for clarity.

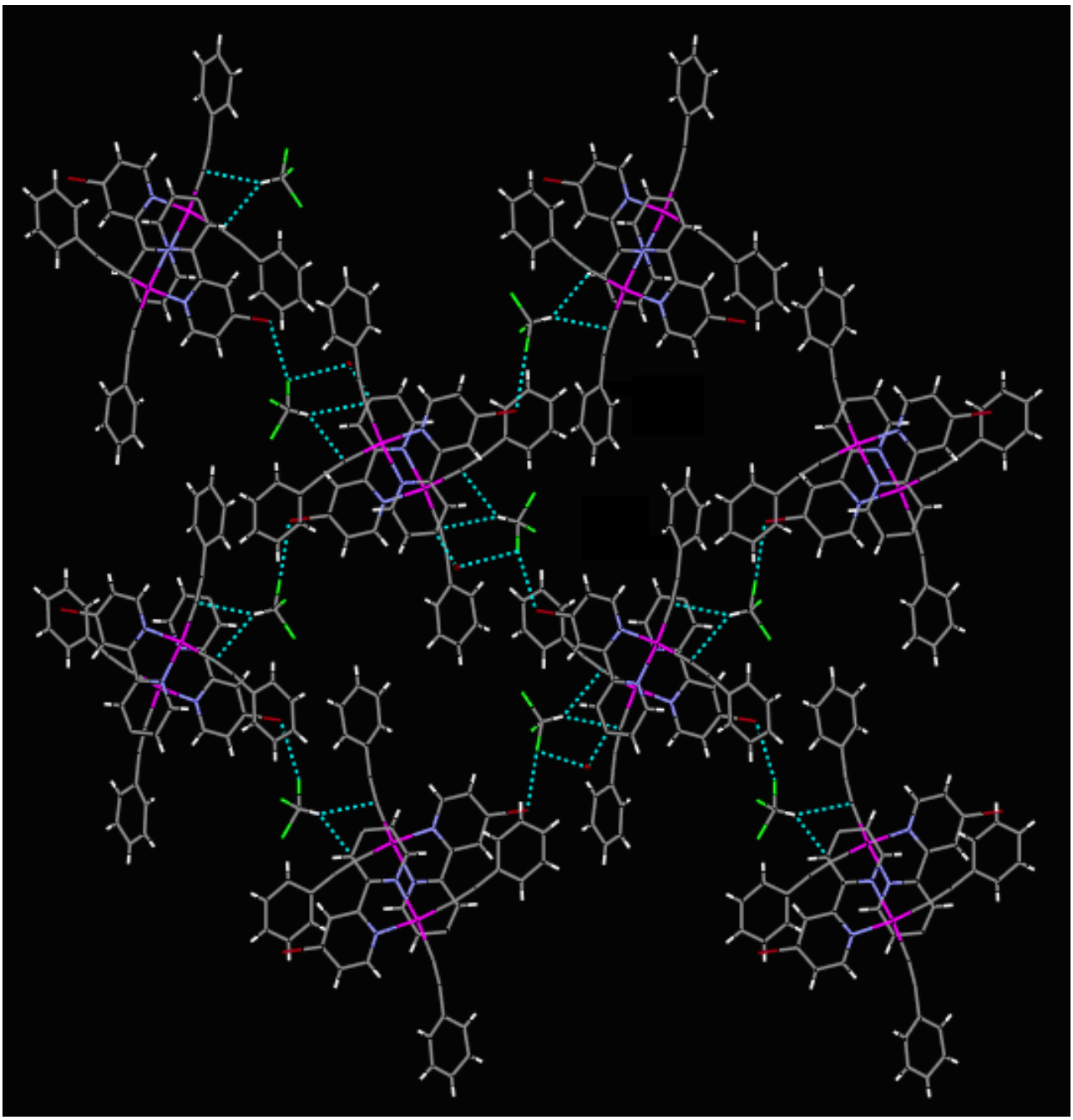

Figure S2. The Pt moiety plane in **1**·2($CHCl_3$), observed from *a* axis direction.

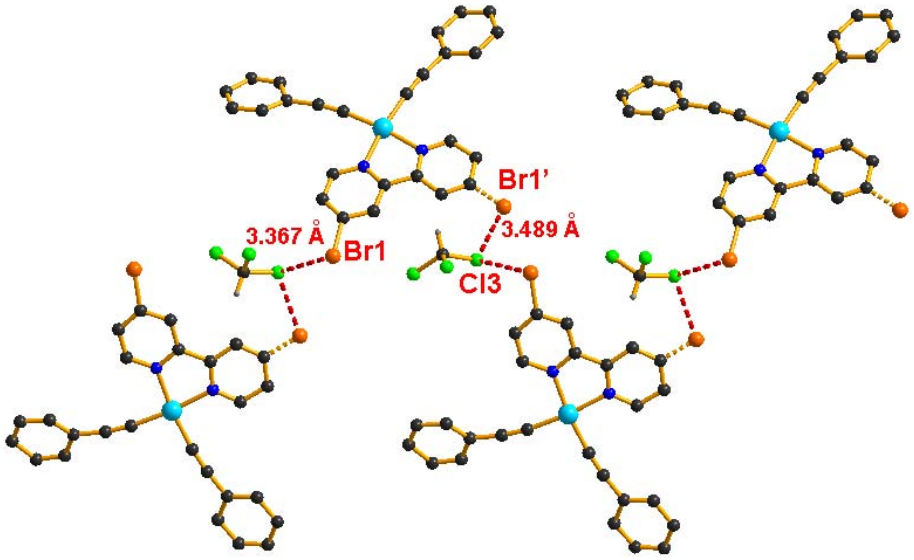

Figure S3. The Br···Cl interactions between platinum moieties and solvate $CHCl_3$ molecules in **1**·2($CHCl_3$). Hydrogen atoms on platinum moieties are omitted for clarity.

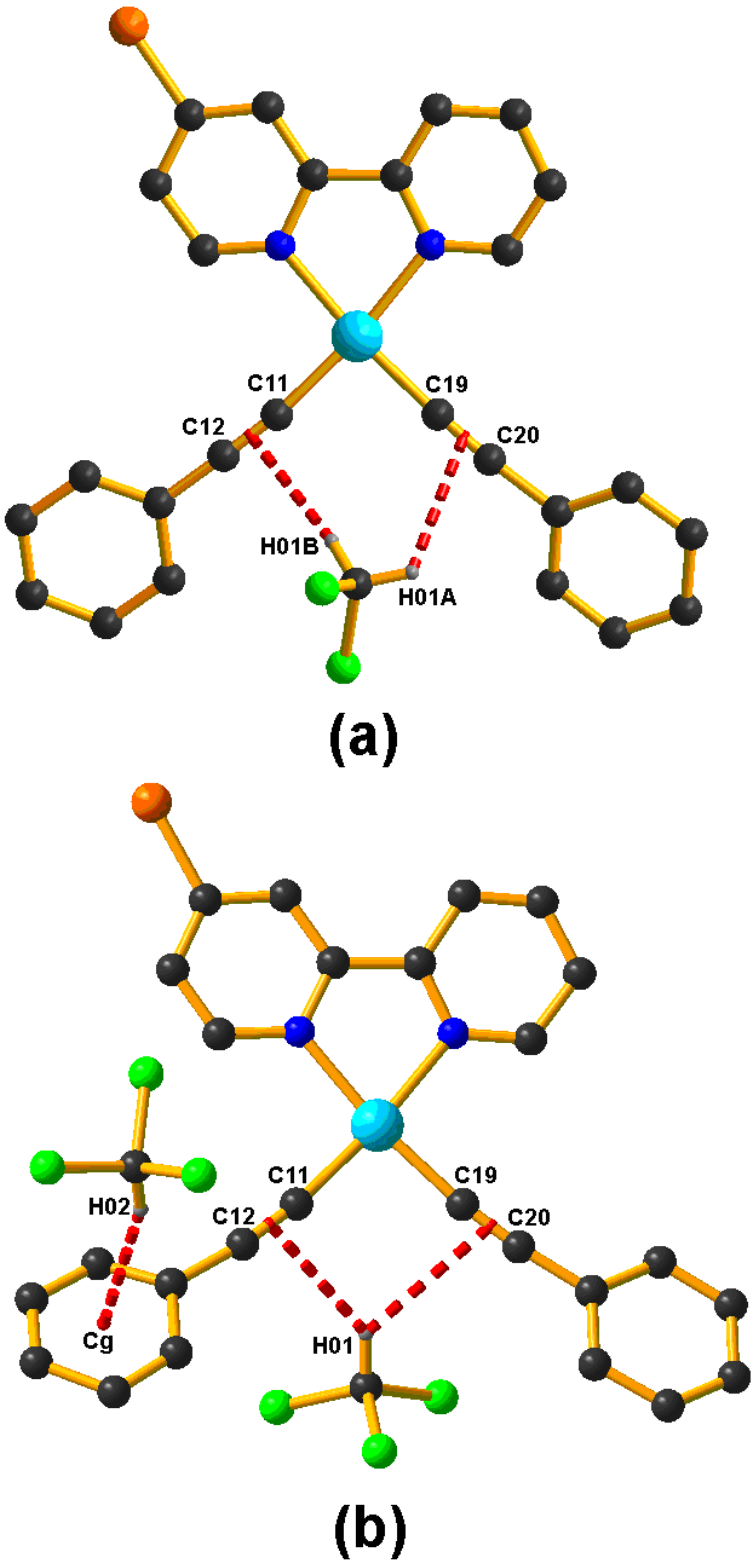

Figure S4. The hydrogen bonds between solvate molecules and platinum moieties in **1**·2(CH_2Cl_2) (a) and **1**·2($CHCl_3$) (b). Hydrogen atoms not participating in the hydrogen bonds are omitted for clarity.

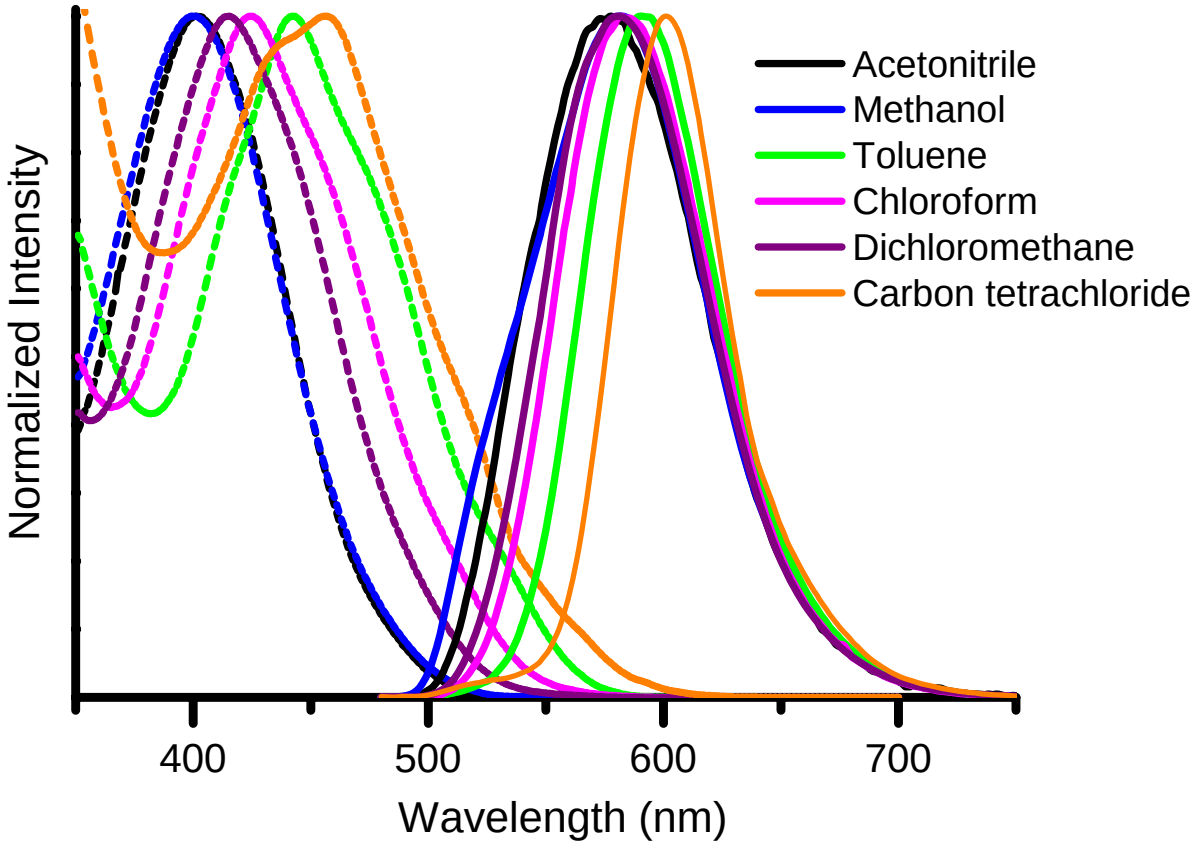

Figure S5. Low-energy absorption (dash lines) and emission spectra (solid lines) of **1** in various solvents at ambient temperature.

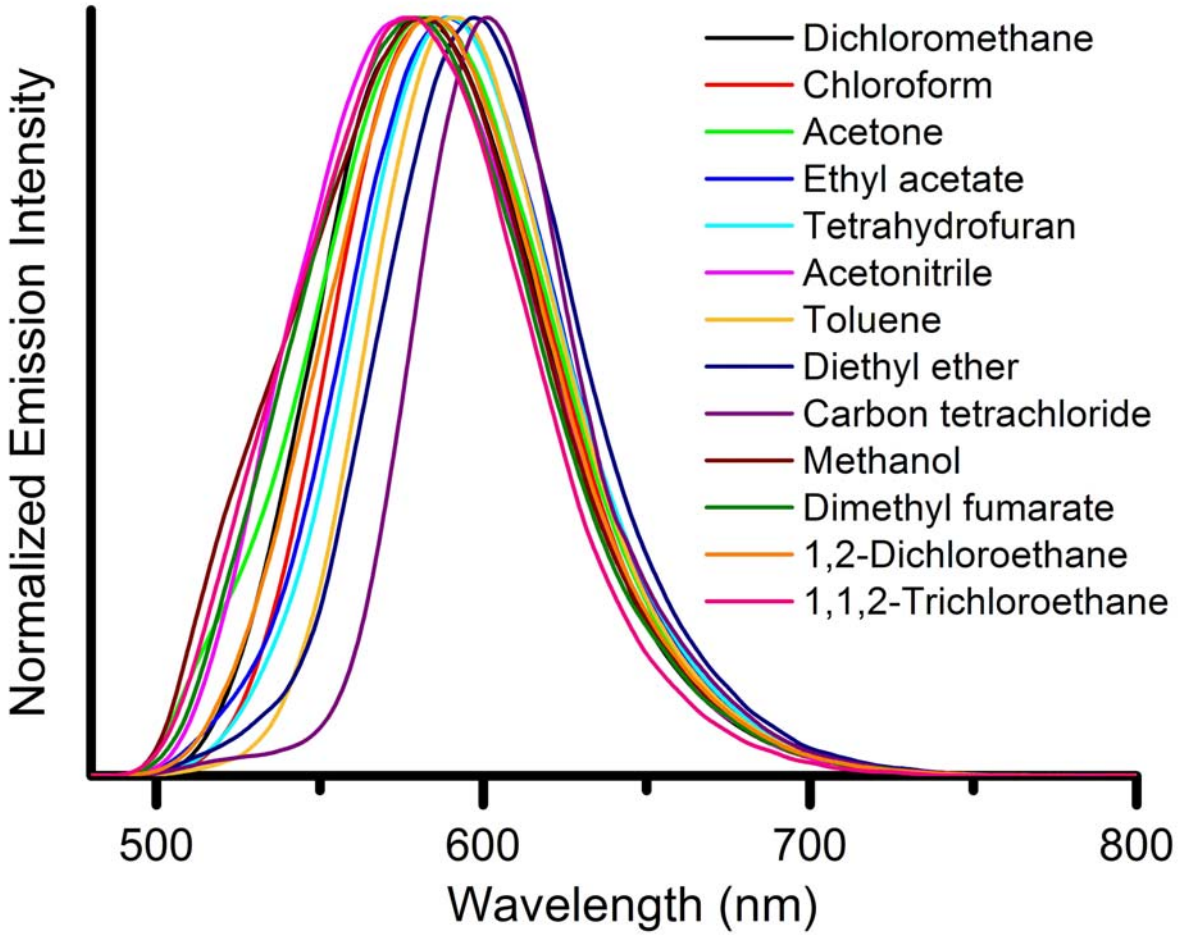

Figure S6. Liquid state emission spectra of **1** in various solvents at ambient temperature.

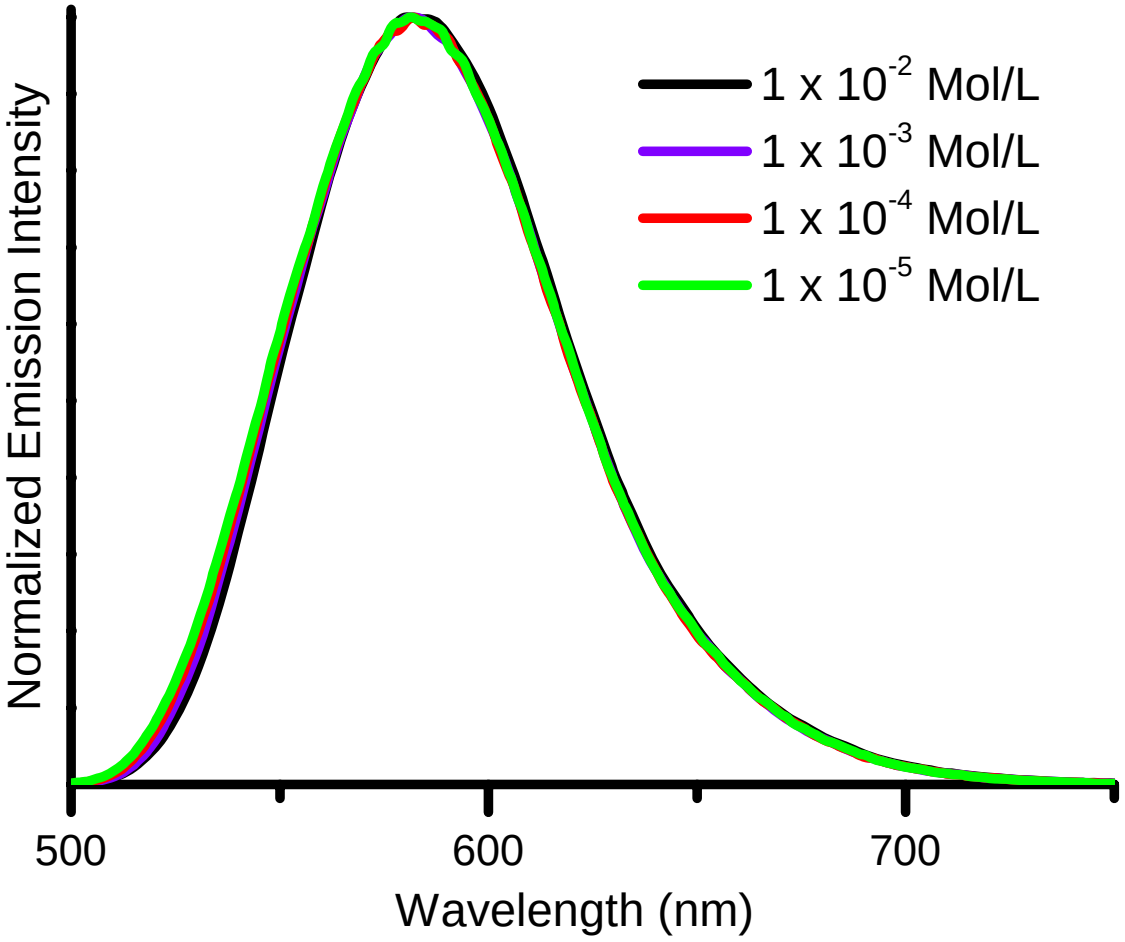

Figure S7. Liquid state emission spectra of **1** in CH_2Cl_2 solution with different concentration at ambient temperature.

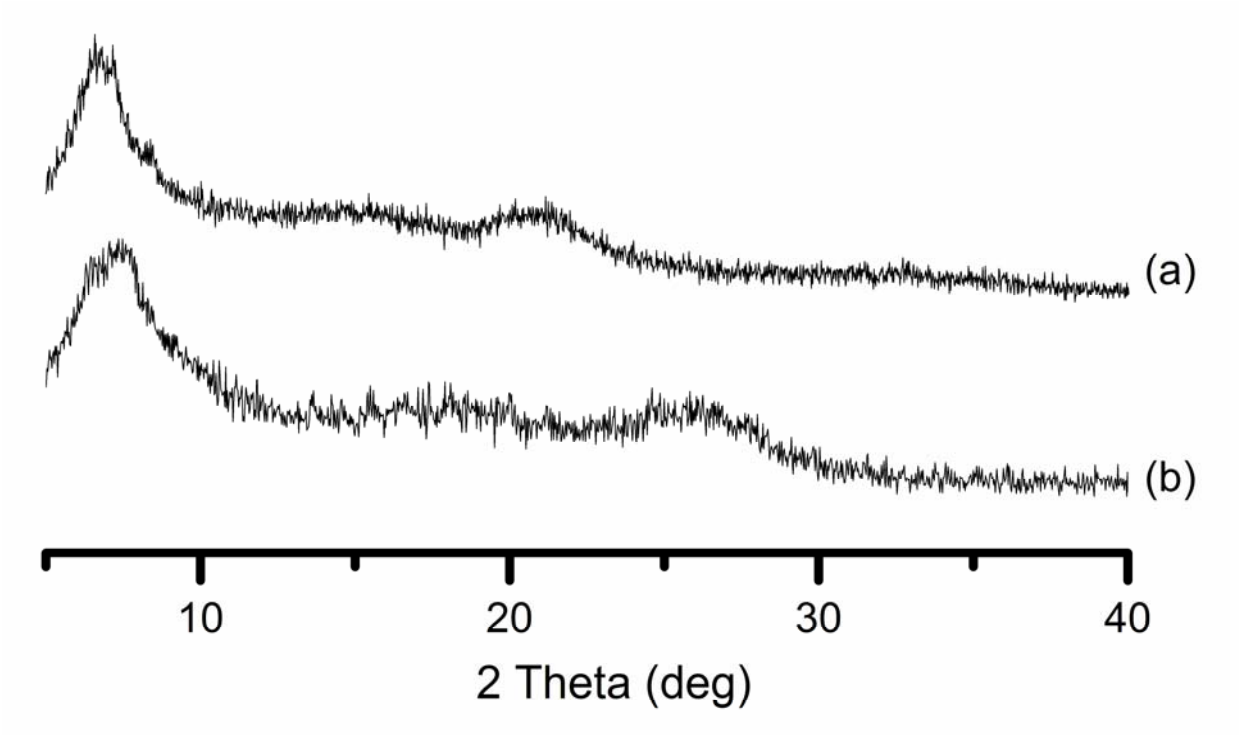

Figure S8. The XRD diagrams of (a) **1**·2(CH_2Cl_2) and (b) **1**·2($CHCl_3$) after heated at 100ºC for 1 hour.

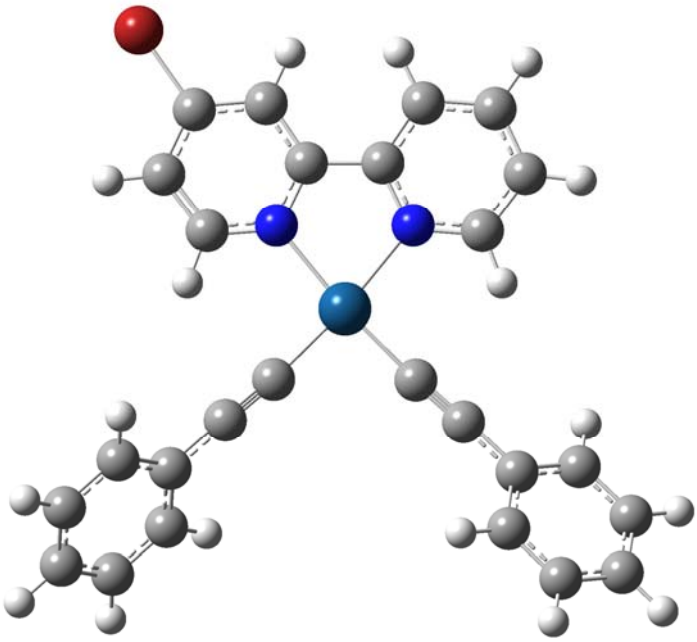

Figure S9. Optimized structure of **1** in the ground state by DFT method at the PBE1PBE level.

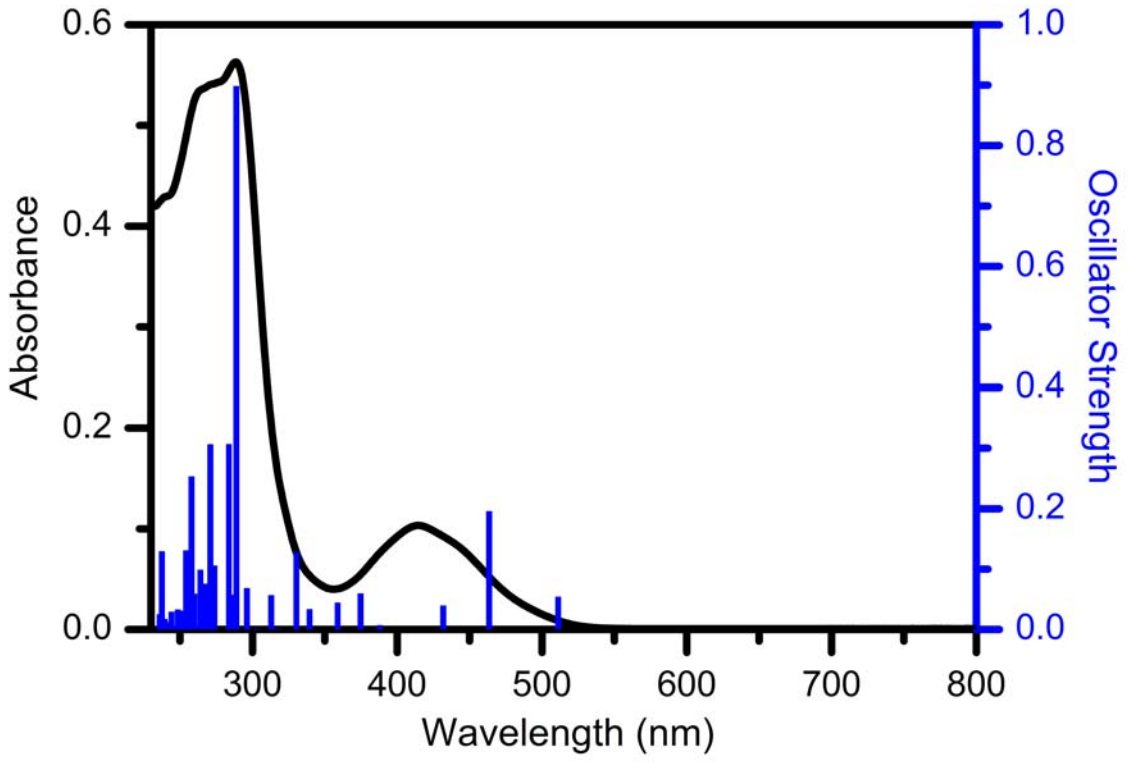

Figure S10. Calculated (blue vertical bars) and measured (black line) UV-vis absorption spectra of **1** in dichloromethane solution at ambient temperature.

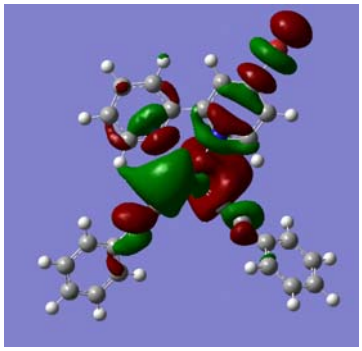

LUMO+10

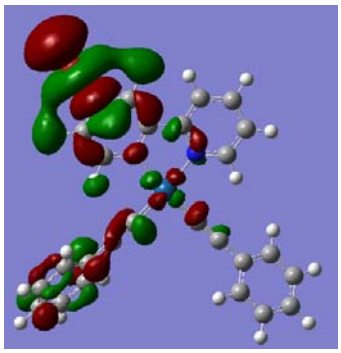

LUMO+5

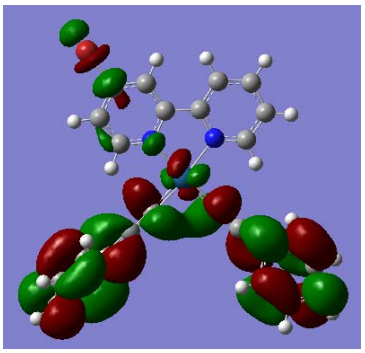

LUMO+4

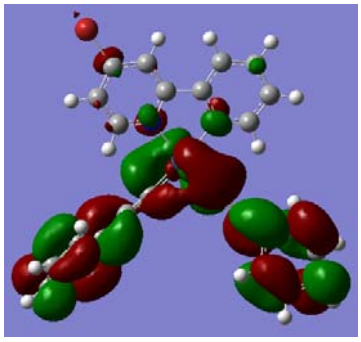

LUMO+3

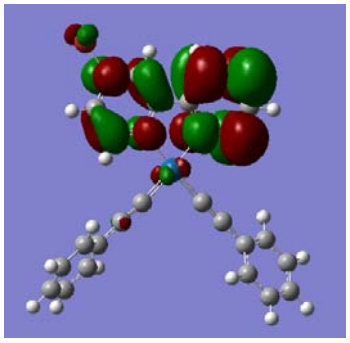

LUMO+2

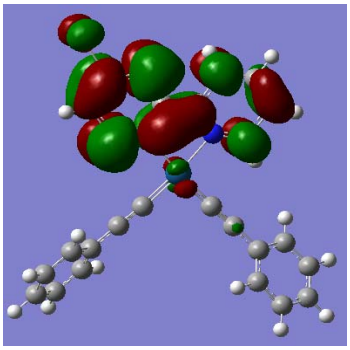

LUMO+1

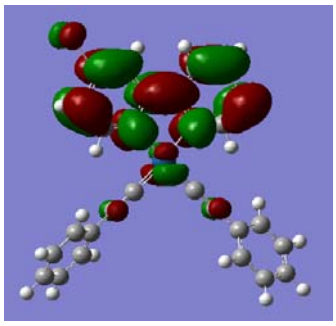

LUMO

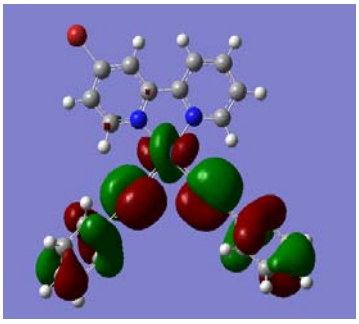

HOMO

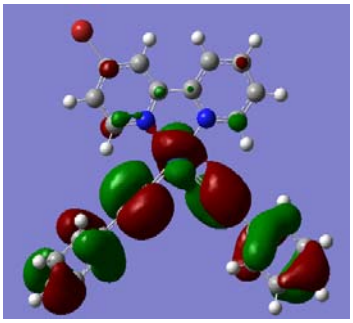

HOMO-1

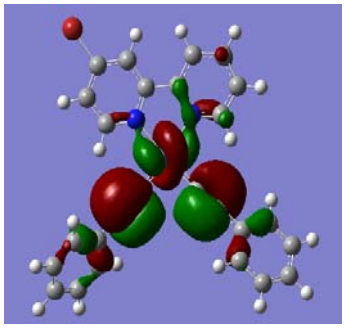

HOMO-2

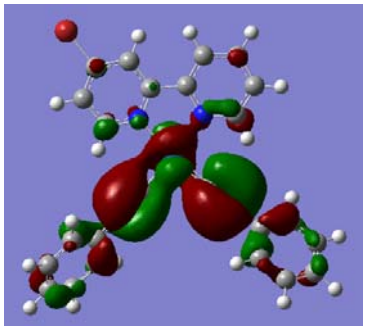

HOMO-3

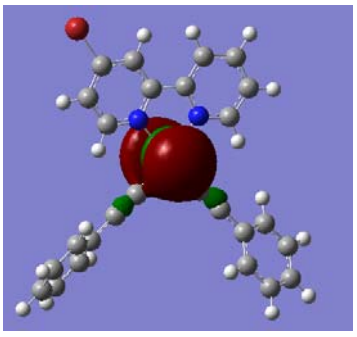

HOMO-4

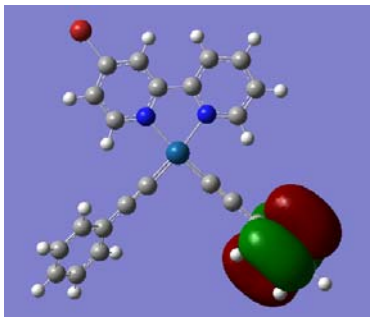

HOMO-5

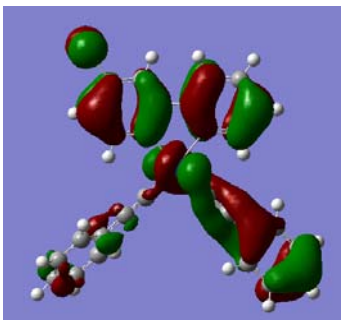

HOMO-7

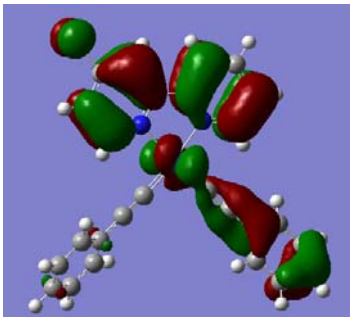

HOMO-8

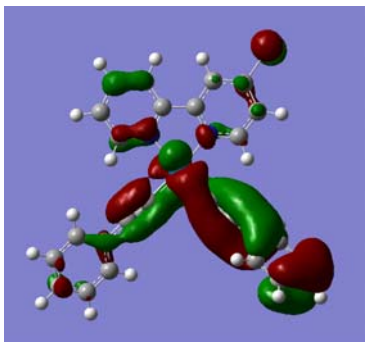

HOMO-9

Figure S11. Plots of the frontier molecular orbitals involved in the absorption of **1** in dichloromethane solution (isovalue = 0.02).

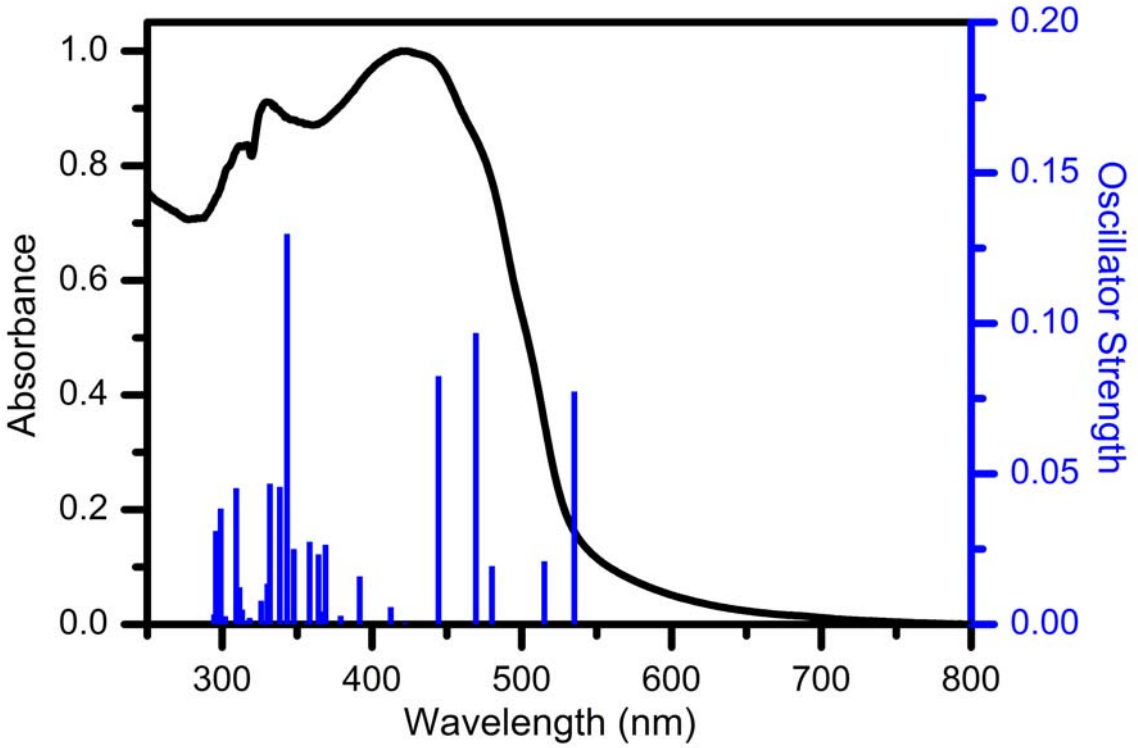

Figure S12. Calculated (blue vertical bars) and measured (black line) UV-vis absorption spectra of solid state **1**·2(CH_2Cl_2) at ambient temperature.

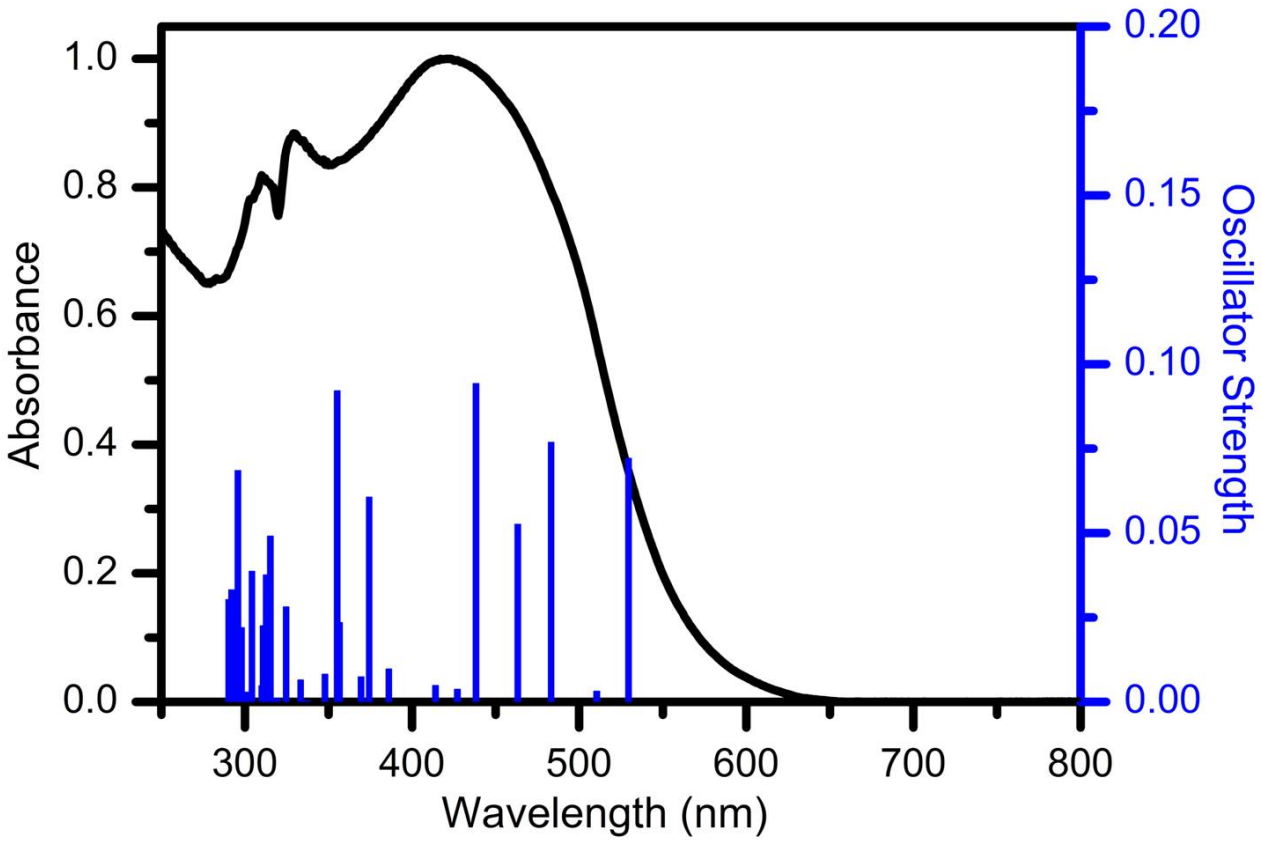

Figure S13. Calculated (blue vertical bars) and measured (black line) UV-vis absorption spectra of solid state **1**·2($CHCl_3$) at ambient temperature.

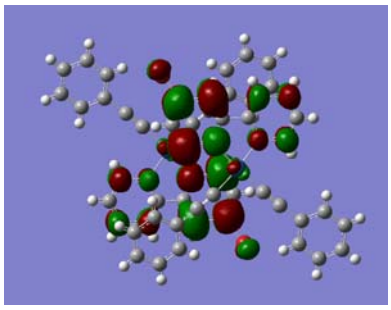

LUMO+5

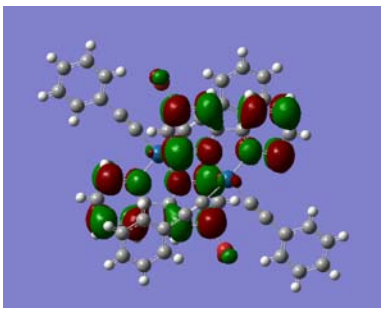

LUMO+4

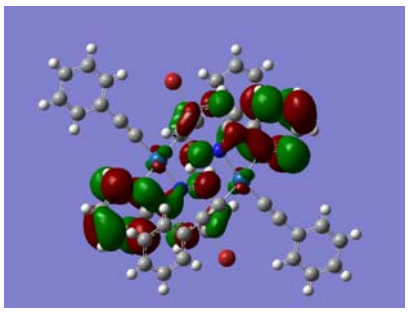

LUMO+3

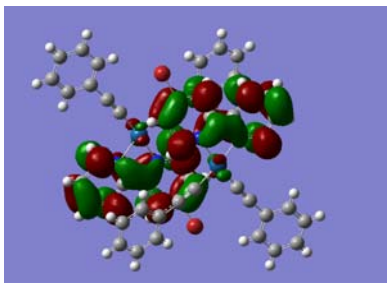

LUMO+2

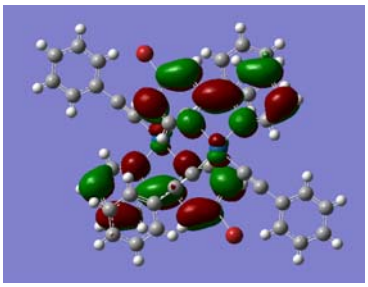

LUMO+1

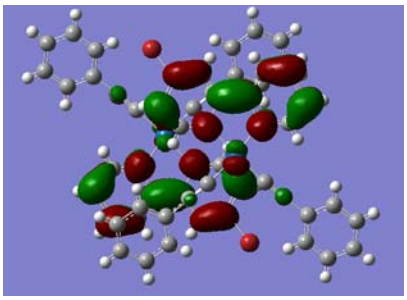

LUMO

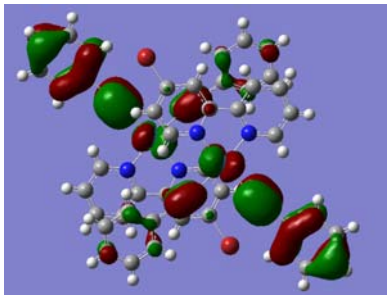

HOMO

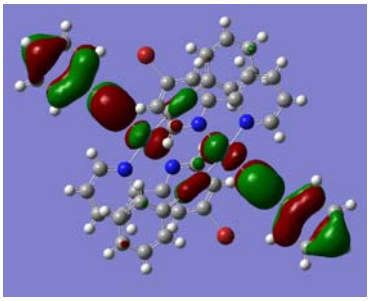

HOMO-1

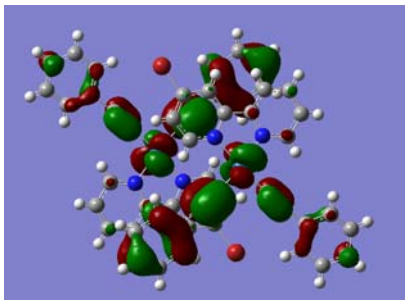

HOMO-2

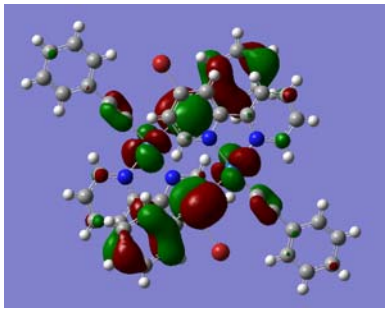

HOMO-3

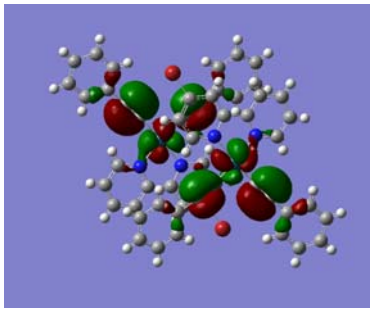

HOMO-4

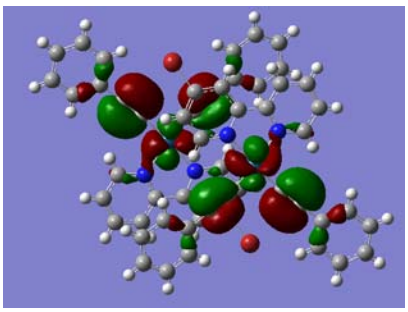

HOMO-5

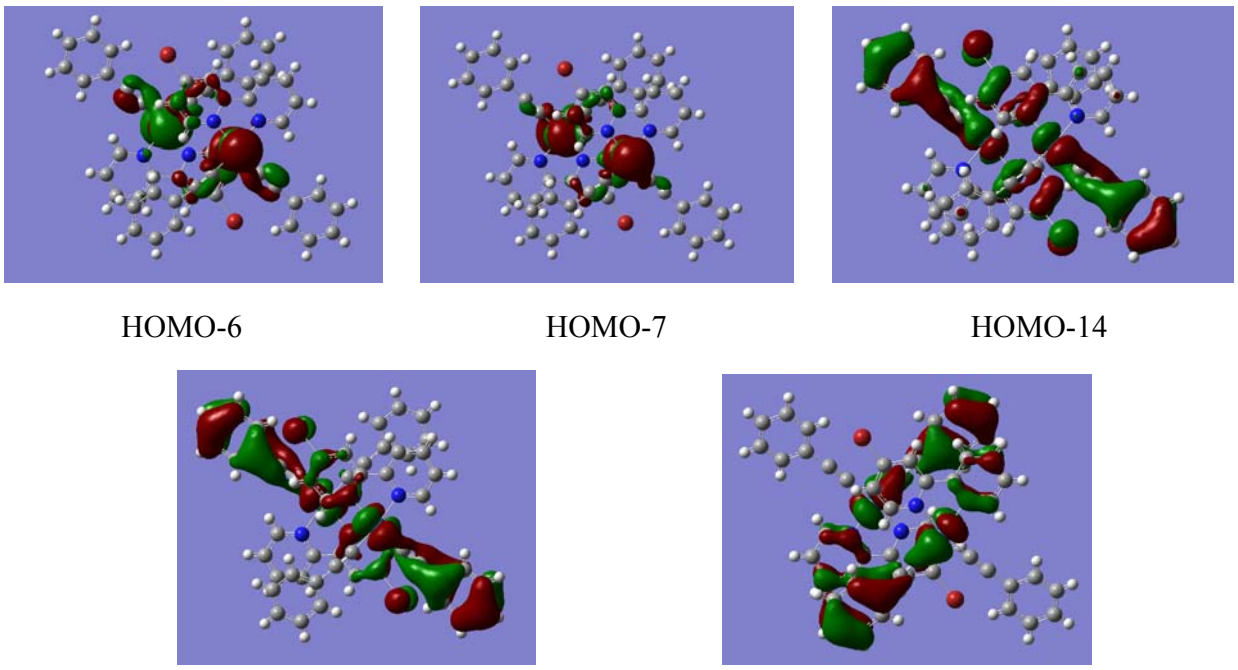

Figure S14. Plots of the frontier molecular orbitals involved in the absorption of **1**·2(CH_2Cl_2) in solid state (isovalue = 0.02).

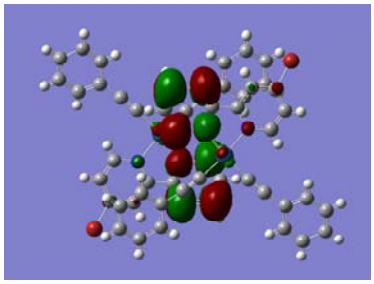

LUMO+5

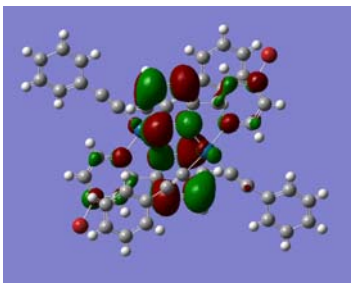

LUMO+4

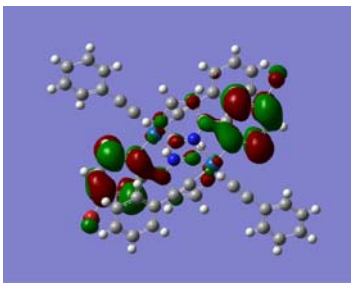

LUMO+3

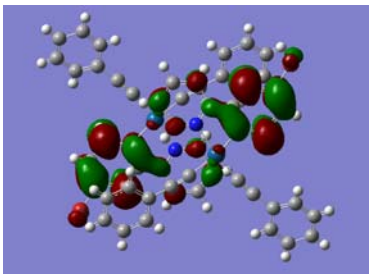

LUMO+2

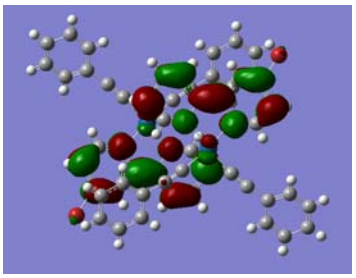

LUMO+1

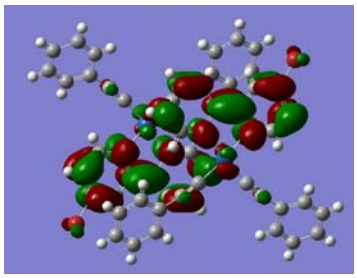

LUMO

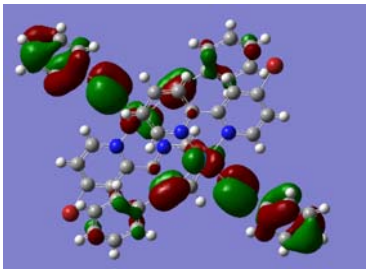

HOMO

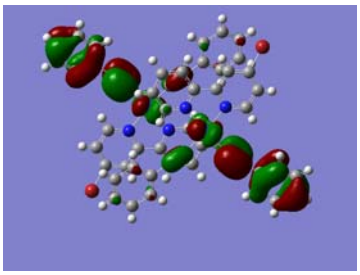

HOMO-1

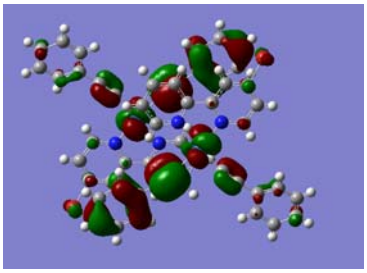

HOMO-2

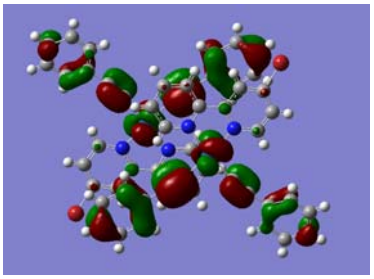

HOMO-3

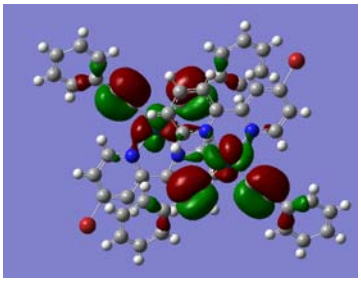

HOMO-4

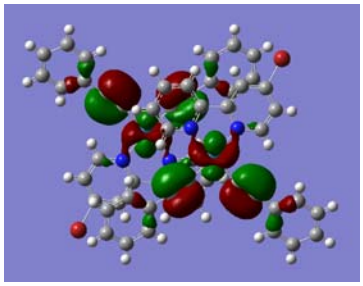

HOMO-5

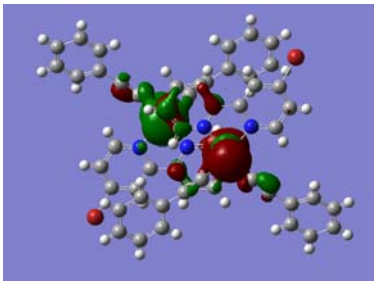

HOMO-6

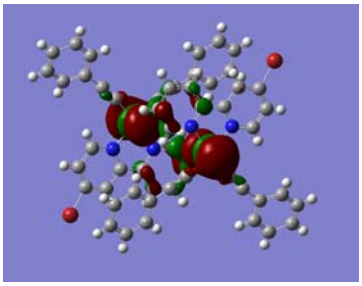

HOMO-7

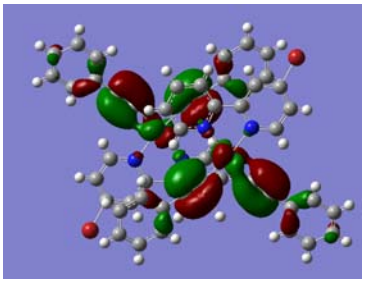

HOMO-9

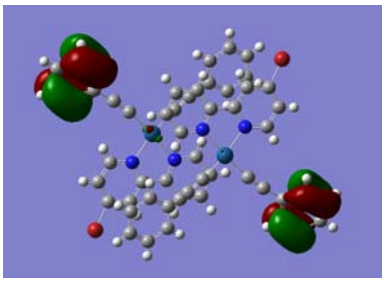

HOMO-12

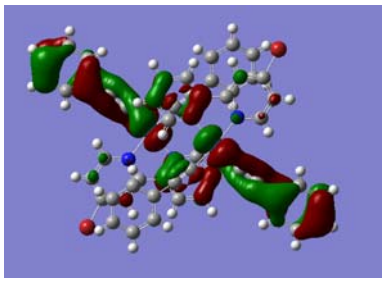

HOMO-14

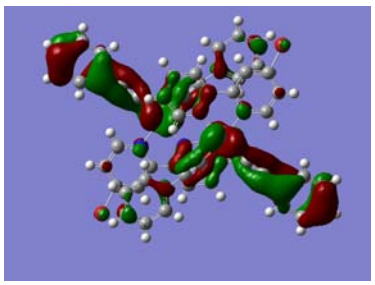

HOMO-16

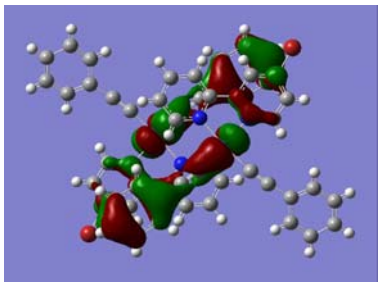

HOMO-17

Figure S15. Plots of the frontier molecular orbitals involved in the absorption of **1**·2($CHCl_3$) in solid state (isovalue = 0.02).

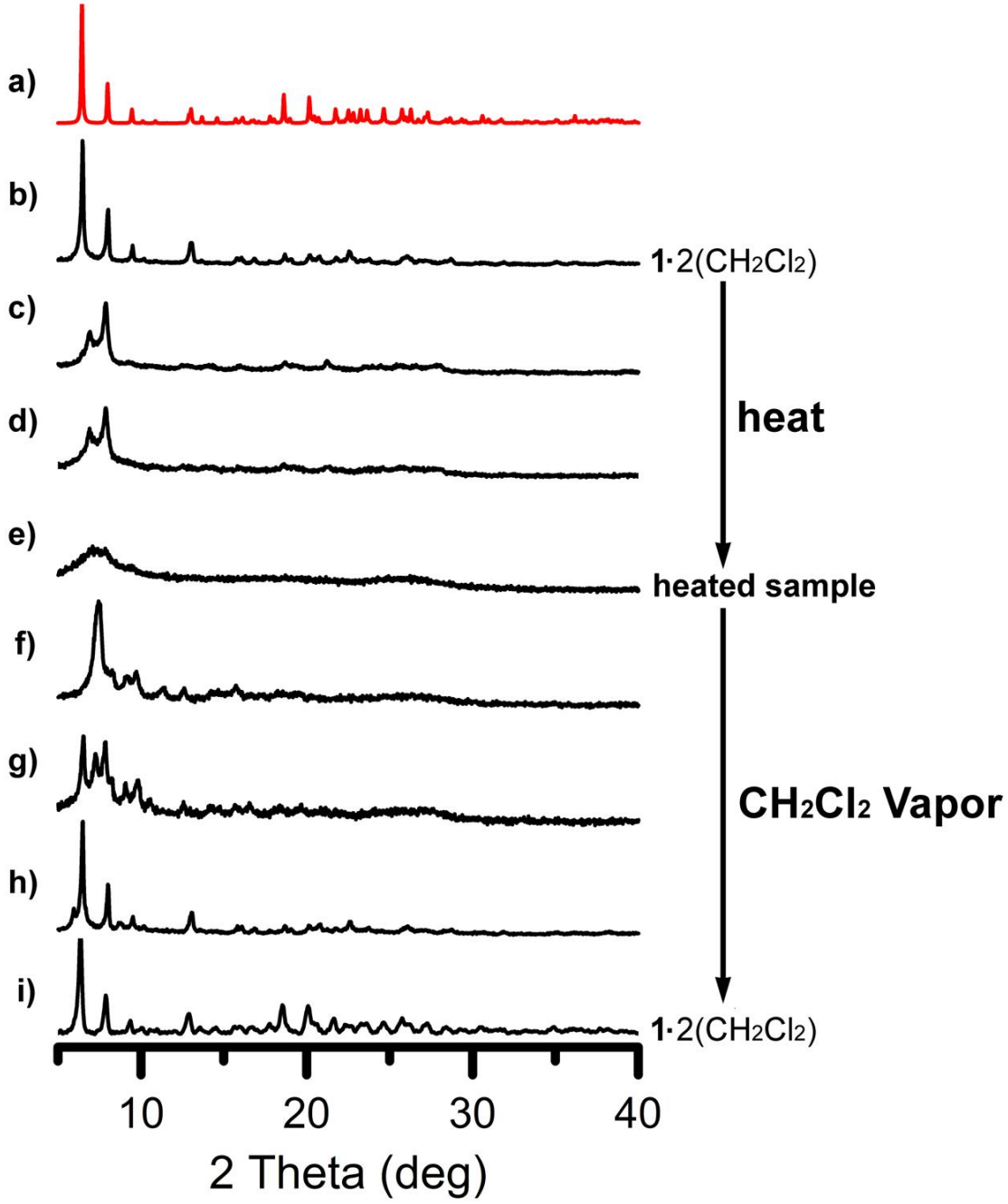

Figure S16. The XRD diagrams recorded in a reversible heating-absorbing cycle, showing dynamic variations of XRD patterns from b)-e) in the heating process of **1**·2(CH_2Cl_2), and the XRD patterns from e)-i) in the reversed process by exposing heated sample into CH_2Cl_2 vapor at ambient temperature. a) The simulated pattern of **1**·2(CH_2Cl_2).

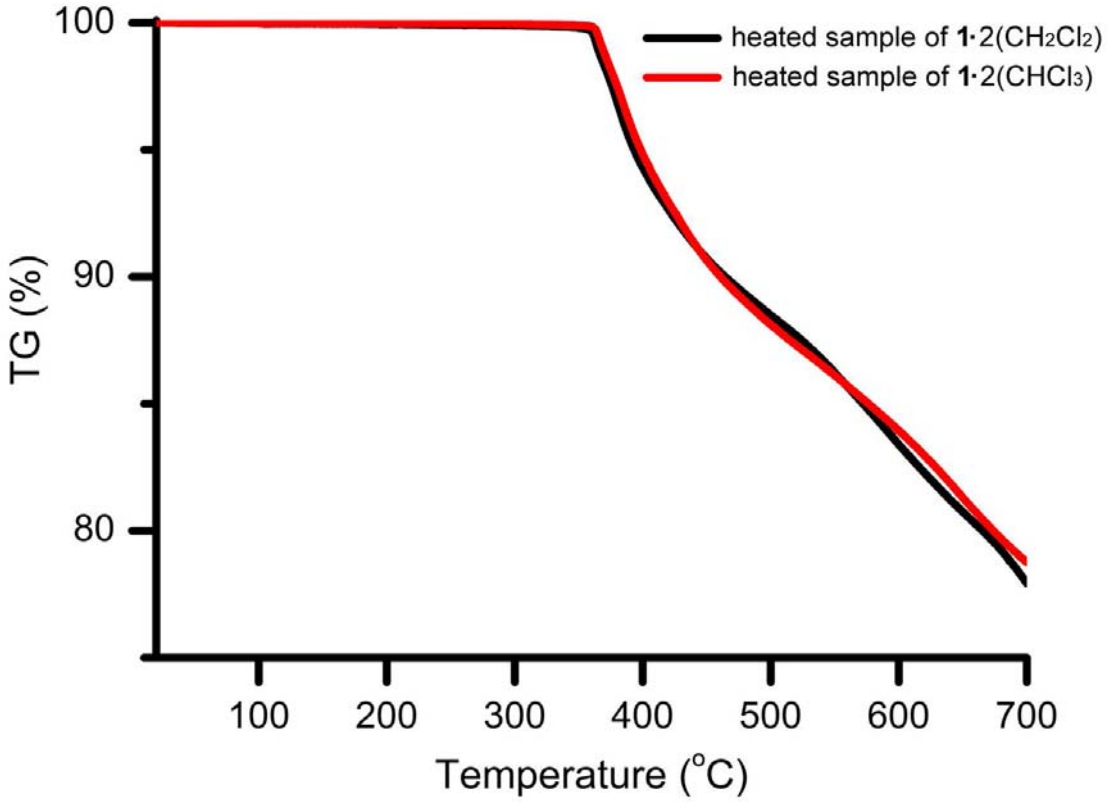

Figure S17. Thermogravimetric analysis curves of crystalline species **1**·2(CH_2Cl_2) and **1**·2($CHCl_3$) after heated at 100ºC for 1 hour.

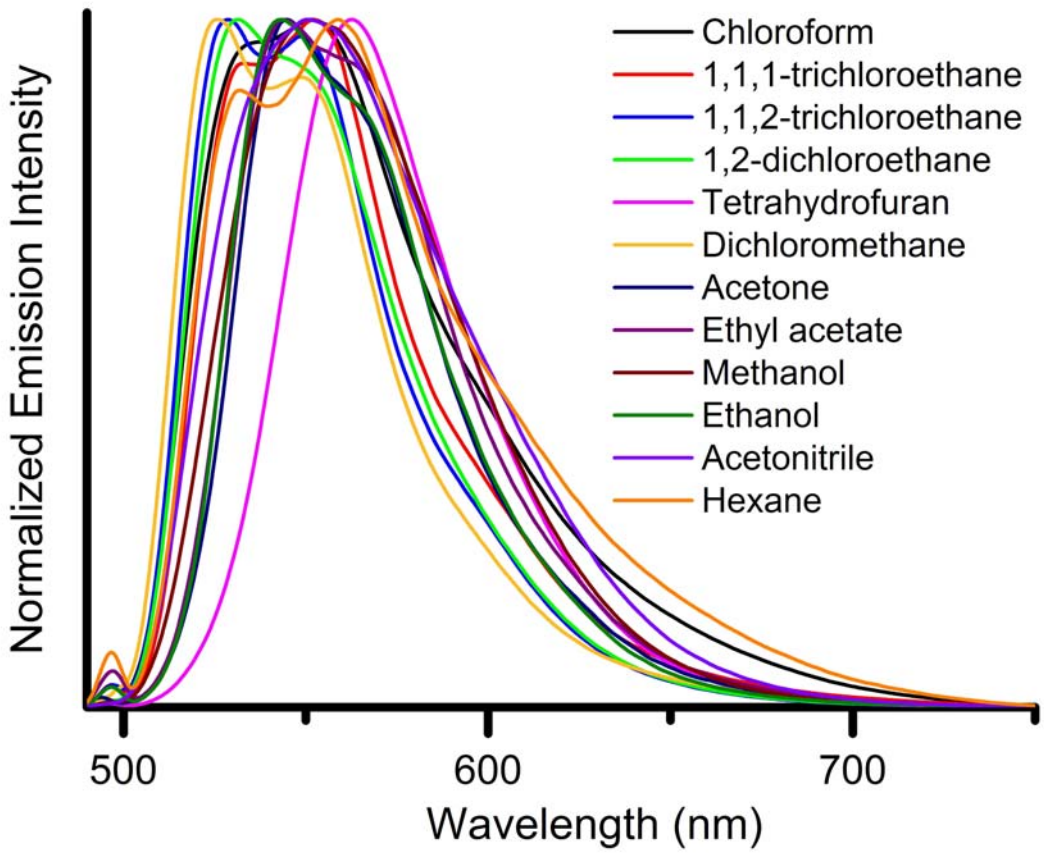

Figure S18. Emission spectra of ground sample **1** upon exposure to various VOC vapors at ambient temperature.

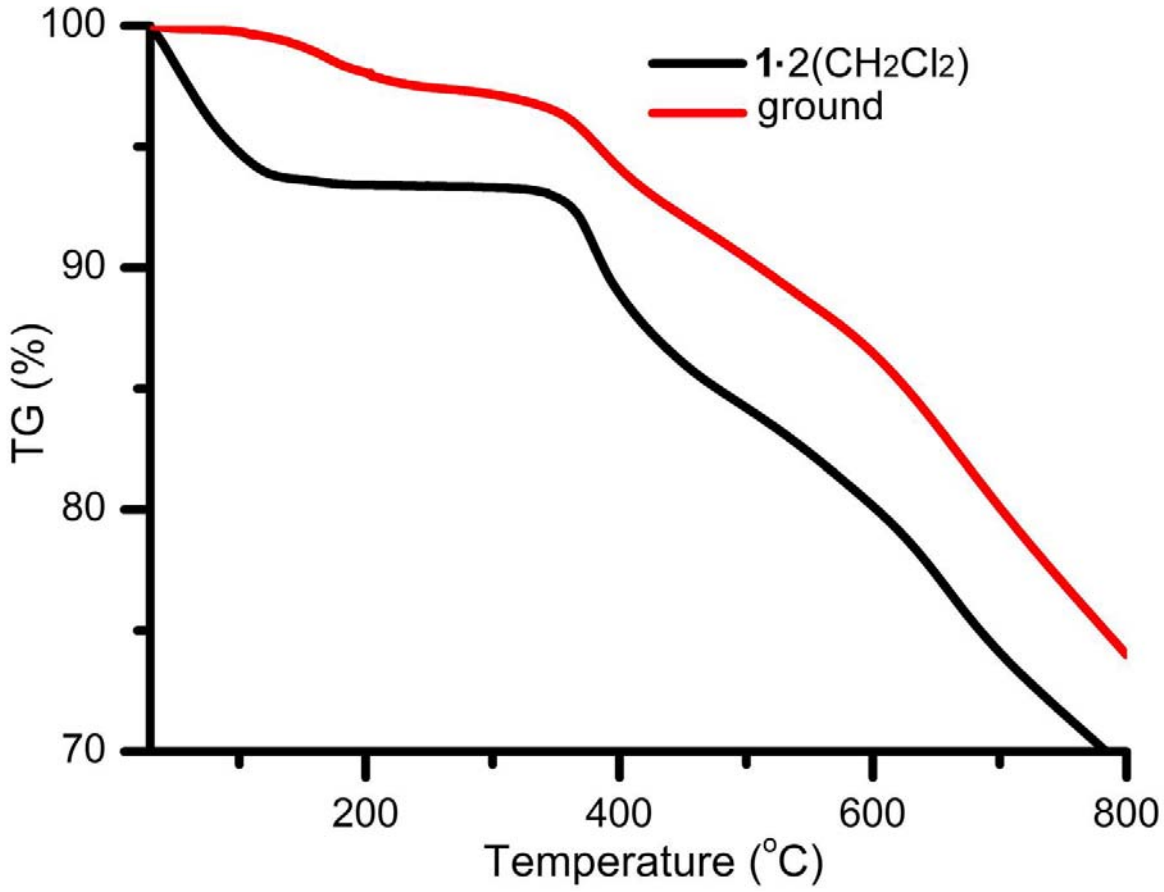

Figure S19. Thermogravimetric analysis curves of crystalline **1**·2(CH_2Cl_2) (black) and the corresponding ground species (red).

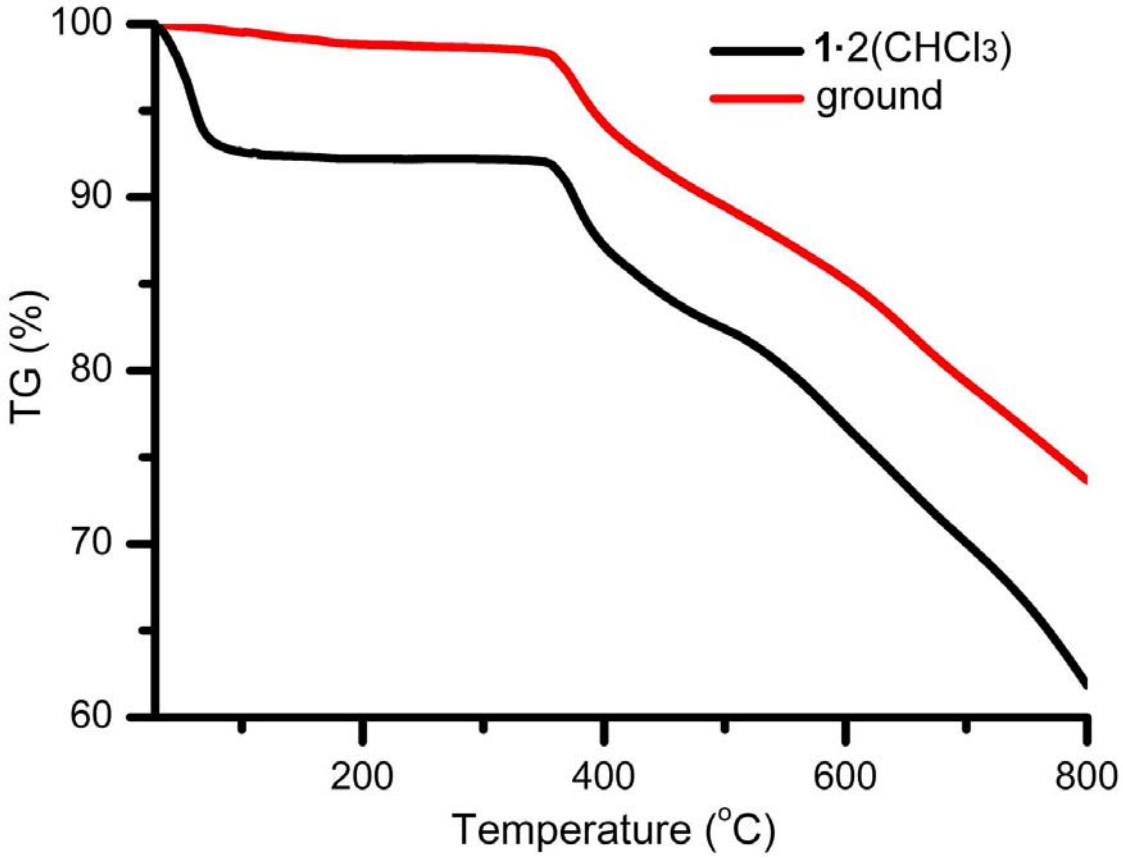

Figure S20. Thermogravimetric analysis curves of crystalline **1**·2($CHCl_3$) (black) and the corresponding ground species (red).

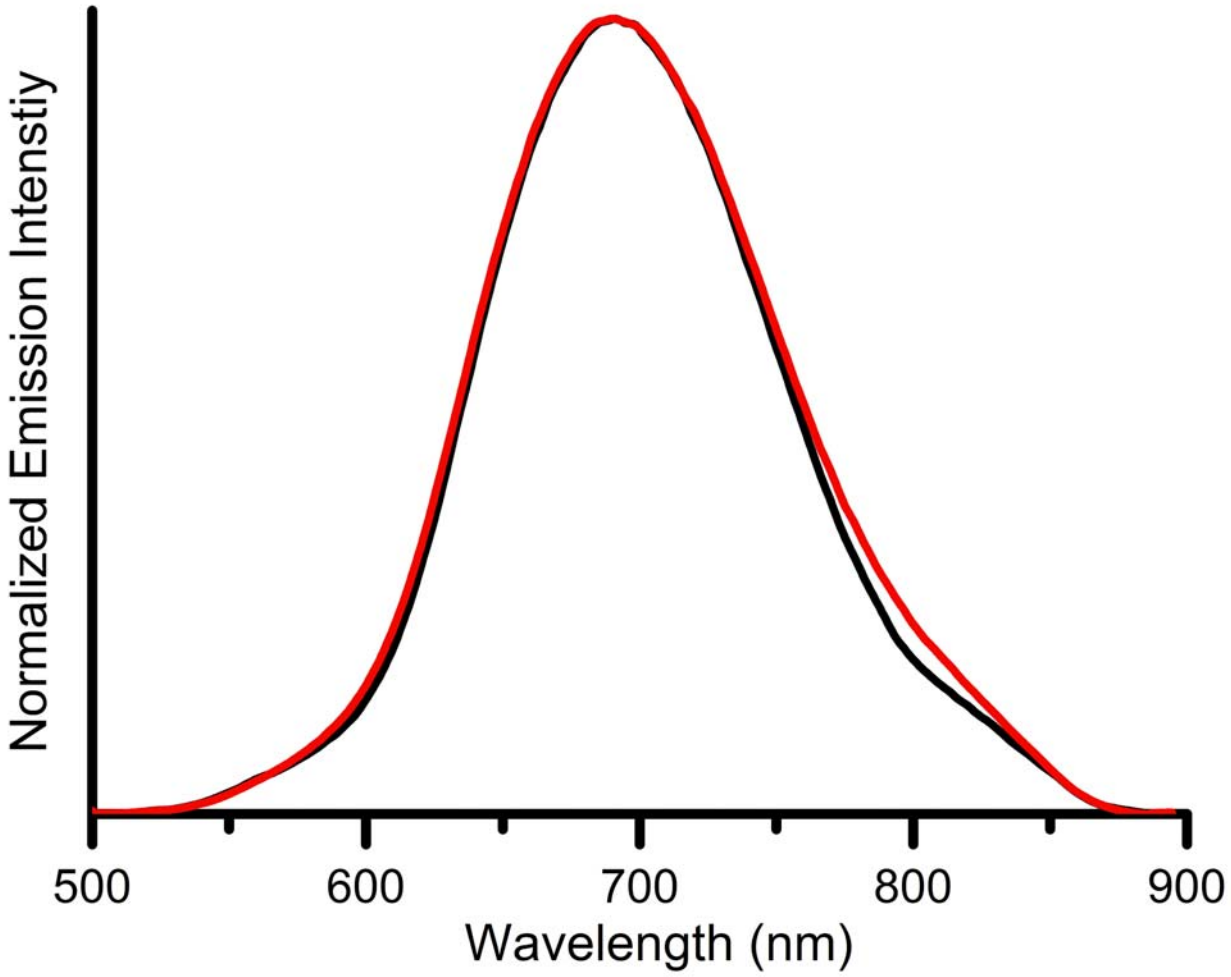

Figure S21. The emission spectra of heated-sample of **1**·2(CH_2Cl_2) after ground and heated-sample of **1**·2($CHCl_3$) after ground (red line).